# Analysis of Human Buccal Absorption of Drugs by Physical Model Approach

K. R. M. VORA▲, W. I. HIGUCHI, and N. F. H. HO

**Abstract** □ The studies of Beckett and Moffat on the human buccal absorption of *p-n*-alkyl phenylacetic, *p*-halogen phenylacetic, and toluic acids at various buffer pH's were analyzed quantitatively by the physical model approach using a two-phase compartmental diffusion model. Nonlinear regression analysis was used to obtain self-consistent estimates of relevant transport parameters such as the permeabilities of the aqueous diffusion layer and lipoidal membrane and the pKa. Good agreement of the absorption rate–buffer pH profiles between the experimental results and theory was found. The incremental partition constant of the lipoidal biophase for a methylene group with the *p*-alkyl phenylacetic acid series was found to be 2.22, in agreement with 2.33 obtained previously for the *n*-alkanoic acids. Halogen substituent constants on the *para*-position of phenylacetic acid and position constants of a methyl group on the *para*-, *meta*-, and *ortho*-positions of benzoic acid relative to aqueous–buccal membrane partitioning were also determined. After comparing these constants with those in the literature, it appears that the rate-determining environment in the lipoidal buccal membrane has a polarity like isobutanol.

**Keyphrases** □ Buccal absorption—*p-n*-alkyl phenylacetic, *p*-halogen phenylacetic, and toluic acids, application of partition coefficients □ Absorption, buccal—*p-n*-alkyl phenylacetic, *p*-halogen phenylacetic, and toluic acids, application of partition coefficients □ Phenylacetic acids, *p-n*-alkyl and *p*-halogen—application of partition coefficients to buccal absorption □ Toluic acids—application of partition coefficients to buccal absorption □ Partition coefficients—application to buccal absorption

Recently, the use of the physical model approach to the quantitative interpretation of the *in vivo* buccal absorption of *n*-alkanoic acids was demonstrated (1). The buccal absorption data of Beckett and Moffat (2) were utilized in these model calculations. Exceptionally good agreement of the absorption rate–buffer pH profiles between the experimental results and theory was found. The greater rates of absorption of the higher molecular weight acids in the homologous series at constant buffer pH of the drug solution were attributed entirely to the higher partition coefficients for these acids because their pKa values are essentially identical. However, the rightward shifts of the profiles of the homologous series relative to the dissociation curve were attributed not only to the increasing lipid solubility but also to the presence of an aqueous diffusion layer on the mucosal side of a biphasic aqueous–lipid barrier. The permeability of the aqueous diffusion layer (stagnant layer) was the rate-controlling factor for the maximum rates observed at the low pH region for the higher alkanoic acids within the homologous series. A self-consistent, biophysically meaningful factor of 2.33 for the buccal lipoidal membrane–aqueous incremental partition constant for a methylene group was found. Since the incremental partition constant was less than 3.15, as found in the octanol–water system, it was further implied that the buccal membrane was effectively more polar. Consequently, *in vitro* partitioning data with the isobutanol–water system, such as those reported by Collander (3), may provide better correlation with the buccal absorption data than the hexane–water, the octanol–water, or the *n*-heptane–aqueous partition coefficients.

The purpose of this paper is to demonstrate the application of the above-mentioned diffusion model to additional *in vivo* buccal absorption data of Beckett and Moffat (2, 4) involving the following series of compounds: *p-n*-alkyl phenylacetic acids, *p*-halogen phenylacetic acids, and toluic acids. These compounds were selected because they represent a series of drugs having relatively the same pKa with different lipid solubility or different pKa with different lipid solubility. It also will be shown that these sets of compounds may provide incremental partition constants for the methylene group within a homologous linear alkyl chain, substituent constants for the various halogens on the *para*-position of phenylacetic acid, and position constants for methyl groups on benzoic acid.

## DESCRIPTION OF MODEL

The diffusion model related to buccal absorption is a two-compartment model. The first compartment (mucosal side) consists of the bulk aqueous drug solution phase and a diffusion layer of thickness $L_1$, and it is in series with the second compartment consisting of a homogeneous lipid phase of thickness $L_2$. It is assumed that there is a perfect sink on the serosal side after the lipid phase and that only nonionized drug species transfer across the lipid membrane.

The equations describing the steady-state first-order rate of buccal absorption (1) are summarized as follows:

$$K_u = B_1 \cdot f(T) \qquad \text{(Eq. 1)}$$

where:

$$B_1 = \frac{AP_{w,1}}{V} \qquad \text{(Eq. 2)}$$

$$f(T) = \frac{1}{(1 + K_a/[H^+])T + 1} \qquad \text{(Eq. 3)}$$

$$T = \frac{P_{w,1}}{P_{o,2}} \qquad \text{(Eq. 4)}$$

Here $K_u$ is the absorption rate constant; $B_1$ is a constant with units of time$^{-1}$ and is descriptive of the permeability coefficient of the drug in the aqueous diffusion layer, $P_{w,1}$, the surface area, $A$, and the volume of drug solution, $V$; $f(T)$ is a dimensionless parameter with the limits $0 < f(T) \leq 1$; the diffusion efficiency coefficient, $T$, is the ratio of the permeability coefficients of the drug in the aqueous diffusion layer, $P_{w,1}$, and the lipoidal membrane, $P_{o,2}$; and $K_a$, and $[H^+]$ are the dissociation constant and hydrogen-ion concentration, respectively.

The incremental change in the lipid–aqueous partition coefficient from one compound to the molecular-modified compound within a given series may be generally expressed by:

$$n = \frac{K_{i+1}}{K_i} = \frac{P_{o,2,i+1}}{P_{o,2,i}} = \frac{T_i}{T_{i+1}} \qquad \text{(Eq. 5)}$$

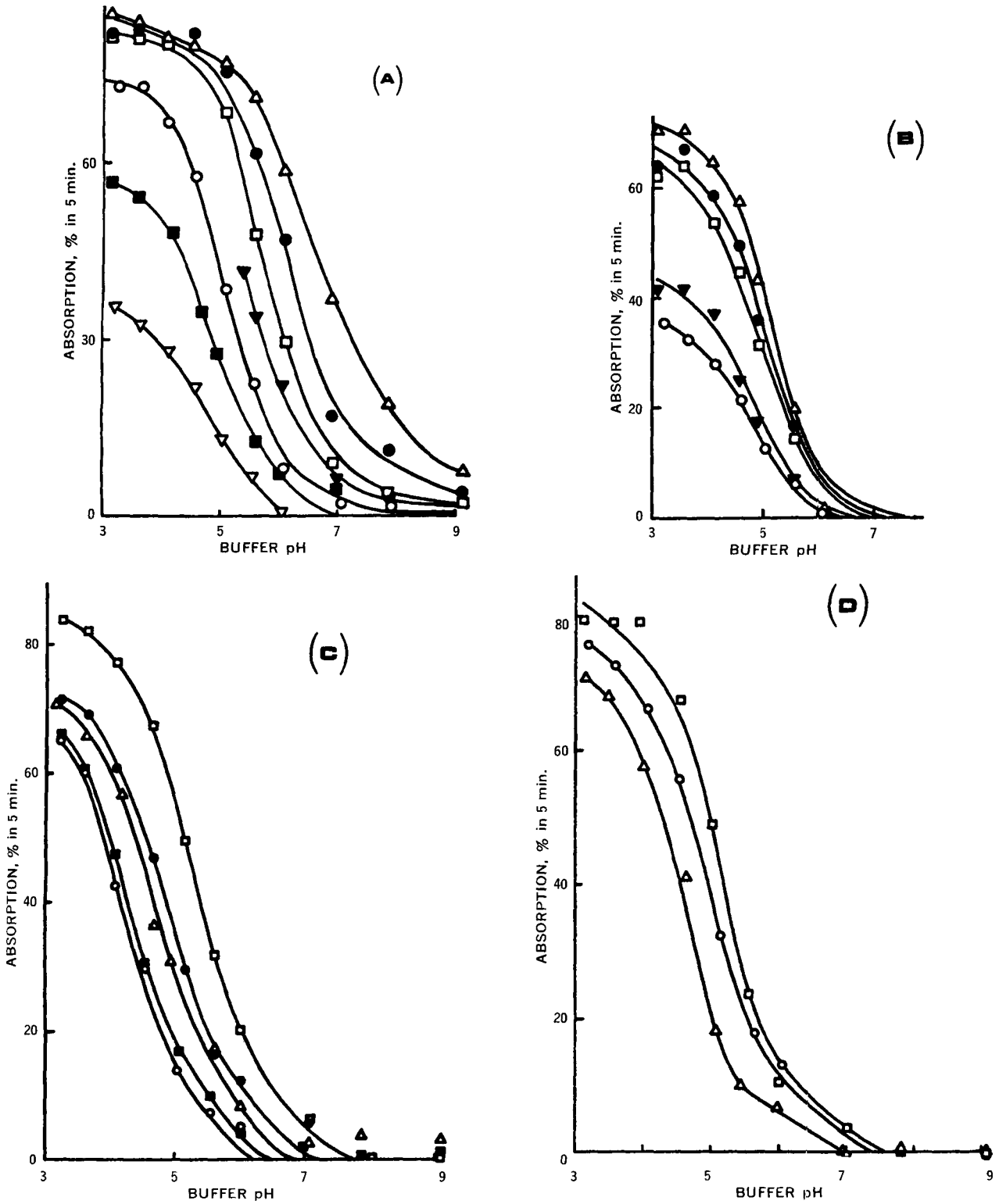


**Figure 1**—*The buccal absorption of acidic drugs in man [from Beckett and Moffat (2, 4)]. (A)* p-n-*Alkyl phenylacetic acids. Key:* △, *hexyl;* ●, *pentyl;* □, *butyl;* ▼, *propyl;* ○, *ethyl;* ■, *methyl; and* ▽, *H. (B)* p-n-*Halogen phenylacetic acids. Key:* △, *iodo;* ●, *bromo;* □, *chloro;* ▼, *fluoro; and* ○, *H. (C) Substituted benzoic acids. Key:* □, *2,4-dimethylbenzoic acid;* ●, m-*toluic acid;* △, *benzoic acid;* ■, *2,4,6-trimethylbenzoic acid; and* ○, *2,3,5,6-tetramethylbenzoic acid. (D) Toluic acids. Key:* □, para; ○, meta; *and* △, ortho.

where $n$ is the lipid–aqueous incremental partition constant, $K$ is the partition coefficient, and the subscripts $i$ and $i+1$ denote the compound and modified compound, respectively.

## RESULTS AND DISCUSSION

The buccal absorption–pH curves involving the passive transfer of *p-n*-alkyl phenylacetic acids, *p*-halogen phenylacetic acids, substituted benzoic acids, and toluic acids are shown in Fig. 1 (2, 4). According to theory, the shape of the absorption rate–pH profile of a drug and between drugs within a data set (for example, the homologous series of the *p-n*-alkyl phenylacetic acids) is related to the various interactions involving the hydrodynamics in the buccal cavity, the pH of the solution, the pKa, and the intrinsic permeability of the membrane. If one is able to quantitate these factors

**Table I**—Best-Fitting $T_{expt}$ and $K_a$ Values Obtained by the Use of the NONLIN Computer Program for Buccal Absorption Data of Phenylacetic and *p*-Alkyl Phenylacetic Acids[a]

| Acid | $B_1$, min.$^{-1}$ 0.322 | 0.366 | 0.393 | 0.460 | 0.599 |
|---|---|---|---|---|---|
| **Best-Fitting $T_{expt}$** | | | | | |
| Phenylacetic | 2.667 | 3.176 | 3.479 | 4.248 | 5.829 |
| *p*-Methylphenylacetic | 0.910 | 1.175 | 1.333 | 1.733 | 2.555 |
| *p*-Ethylphenylacetic | 0.201 | 0.368 | 0.467 | 0.719 | 1.236 |
| *p*-*n*-Propylphenylacetic | 1.154 | 1.451 | 1.633 | 2.072 | 3.007 |
| *p*-*n*-Butylphenylacetic | 0.063 | 0.067 | 0.145 | 0.341 | 0.744 |
| *p*-*n*-Pentylphenylacetic | 0.002 | 0.063 | 0.140 | 0.335 | 0.737 |
| **Best-Fitting $K_a \times 10^5$** | | | | | |
| Phenylacetic | 2.780 | 2.649 | 2.595 | 2.503 | 2.370[b] |
| *p*-Methylphenylacetic | 3.781 | 3.337 | 3.156 | 2.838 | 2.506 |
| *p*-Ethylphenylacetic | 8.185 | 5.084 | 4.296 | 3.268 | 2.478 |
| *p*-*n*-Propylphenylacetic | 0.303 | 0.275 | 0.262 | 0.243 | 0.217[b] |
| *p*-*n*-Butylphenylacetic | 3.632 | 3.853 | 1.925 | 0.962 | 0.573 |
| *p*-*n*-Pentylphenylacetic | 16.542 | 2.020 | 0.962 | 0.477 | 0.281[b] |
| Average $K_a$ of *p*-alkyl phenylacetic acids | 5.199 | 4.092 | 3.126 | 2.356 | 1.852 |

[a] Literature values for $K_a$ at 25° (5): phenylacetic acid, $4.88 \times 10^{-5}$; and *p*-*n*-alkyl phenylacetic acids, $4.27–4.20 \times 10^{-5}$. [b] These values were not included in the averaging of $K_a$ values.

and also to determine the value of the incremental partition constant $n$, then it is conceivable that, given a rate constant at a specific pH, one could generate or predict the rate constant–pH profiles of the parent drug compound and the corresponding molecular-modified parent compounds in the homologous series. Furthermore, since the experimental data in Fig. 1 are involved with the performance of one test individual under identical conditions, it is expected that the hydrodynamic conditions in the buccal cavity would be nearly constant and, correspondingly, the permeability of all the drug compounds across the aqueous diffusion layer would be nearly identical, as will be shown.

While the quantitative analysis of each set of experimental data in Fig. 1 followed the general approach used previously for the *n*-alkanoic acids (1), a more rigorous computational scheme was applied. Mathematical approximations at various values of the $B_1$ constant were utilized to arrive at the best estimates of the function $f(T)$, the $K_a$ of the acidic drugs, and the diffusion efficiency coefficient $T$ of the buccal membrane leading to a reliable value of the incremental partition constant $n$ which is self-consistent with the experimental results.

**Phenylacetic Acid Series**—The group of *p*-*n*-alkyl phenylacetic acids was reported (5) to possess nearly identical pKa values (4.31–4.37 at 25°). Thus, the differences in absorption among these acids were attributed mainly to the differences in the lipid–aqueous partition coefficients (4). The compounds considered in the sequence of approximations included *p*-methyl- to *p*-*n*-pentylphenylacetic acids (Fig. 1A). All experimental data points for these compounds, except those below the 5% absorption level, were included in the calculations. The percent of drug absorbed in 5 min. at the various buffer pH's was reexpressed in terms of the first-order rate constant $K_u$. The order of mathematical approximations carried out is presented in Scheme I.

**Table II**—Best-Fitting $T_{comp}$ Values Obtained by the Use of the NONLIN Computer Program Employing Fixed Average $K_a$ Values for *p*-*n*-Alkyl Phenylacetic Acids, and Corresponding $n$ Values Calculated for a Methylene Group Increment in the *p*-*n*-Alkyl Phenylacetic Acid Series

| Acid | $B_1$, min.$^{-1}$ 0.322 | 0.366 | 0.393 | 0.460 | 0.599 |
|---|---|---|---|---|---|
| **Fixed Average $K_a \times 10^5$** | | | | | |
| *p*-*n*-Alkyl phenylacetic acids | 5.199 | 4.092 | 3.126 | 2.356 | 1.852 |
| **Best-Fitting $T_{comp}$** | | | | | |
| *p*-Methylphenylacetic | 0.817 | 1.105 | 1.336 | 1.814 | 2.729 |
| *p*-Ethylphenylacetic | 0.261 | 0.406 | 0.529 | 0.796 | 1.328 |
| *p*-*n*-Propylphenylacetic | 0.124 | 0.187 | 0.264 | 0.420 | 0.723 |
| *p*-*n*-Butylphenylacetic | 0.036 | 0.064 | 0.100 | 0.214 | 0.543 |
| *p*-*n*-Pentylphenylacetic | 0.016 | 0.034 | 0.058 | 0.144 | 0.420 |
| **Calculated $n$ Values** | | | | | |
| *p*-Methylphenylacetic | | | | | |
| *p*-Ethylphenylacetic | 3.131 | 2.724 | 2.526 | 2.278 | 2.056 |
| *p*-*n*-Propylphenylacetic | 2.100 | 2.165 | 1.998 | 1.895 | 1.837 |
| *p*-*n*-Butylphenylacetic | 3.437 | 2.917 | 2.631 | 1.961 | 1.331 |
| *p*-*n*-Pentylphenylacetic | 2.187 | 1.892 | 1.737 | 1.486 | 1.291 |
| Average $n$ | 2.713 | 2.424 | 2.223 | 1.905 | 1.628 |

*Scheme I—The series of mathematical approximations carried out for the human buccal absorption data involving p-alkyl phenylacetic acids*

Part A: Selection of the best-fitting $T$ and $K_a$ values for each member of the series and determination of the lipid–aqueous incremental constant, $n$, at an estimated $B_1$ value.

Step 1—Calculate $K_u$ from the percent absorbed in 5 min. at the various buffer pH's for each member acid of the series.

↓

Step 2—Calculate $f(T)_{expt}$ for each member acid by Eq. 1 for an estimated $B_1$ value.

↓ NONLIN

Step 3—Compute $T_{expt}$ and $K_a$ values for each member acid using Eq. 3.

↓

Step 4—Calculate average $K_a$.

↓ NONLIN

Step 5—Compute best estimate of $T_{comp}$ for all member acids by Eq. 3 using the average $K_a$.

↓

Step 6—Calculate $n$ from $T_{comp}$ values using Eq. 5; then calculate average $n$.

Part B: Selection of a member acid as the reference compound from the series and subsequent calculations for generating the theoretical $f(T)$ *versus* buffer pH profile for each member acid.

Step 1—Select $T_{comp}$ value of *p*-methylphenylacetic acid (obtained in Step 5 of Part A) as the reference and, using the value of average $n$ (from Step 6 of Part A), calculate $T_{theor}$ for other members of the series (use Eq. 5). Changing the reference $T_{comp}$ each time, obtain four more sets of $T_{theor}$ values as the last compound is *p*-*n*-pentylphenylacetic acid.

↓

Step 2—Calculate $f(T)_{theor}$ for each member acid in each set using $T_{theor}$ values obtained above, the $K_a$ values from Step 4 of Part A, and Eq. 3.

↓

Step 3—Calculate $\sum_{C_1}^{C_6} \sum_{i=1}^{i=n} [f(T)_{theor} - f(T)_{expt}]^2$ for each set of data. Select the set with the minimum sum for the following step.

↓

Step 4—Use the set selected above to plot $f(T)_{theor}$ *versus* buffer pH for each member acid. Plot $f(T)_{expt}$ points on these profiles to demonstrate the closeness of the fit.

To arrive at an initial estimate of $B_1$, it is observed that the percent absorbed in 5 min. at pH $\leq$ 3 reaches approximately 87% maximum absorption for *p*-butylphenylacetic acid and the higher acids in the homologous series. The significance of this observation is indicated by the model. When the permeability of the drug across the lipoidal membrane is sufficiently greater than its permeability across the aqueous diffusion layer, the total transport rate will be essentially aqueous diffusion-controlled, particularly at buffer pH < pKa of the acidic drug. Consequently, the initial estimate of $B_{1,expt}$ is 0.408 min.$^{-1}$, where $B_{1,expt}$ is the $K_u$ value when $f(T) = 1$. Furthermore, the analysis of the data was carried out for a range of $B_1$ corresponding to 80–95% maximum absorption.

As indicated in Part A of Scheme I, nonlinear regression analyses were carried out between Steps 2 and 3 and between Steps 4 and 5. A subroutine DFUNC of the NONLIN program[1] was used on an IBM model 360/67 computer to obtain the best-fitting values of the $K_a$ and/or $T$ parameters mentioned in Eq. 3. The best-fitting $T_{expt}$ and $K_a$ values obtained in Step 3 for certain selected maximum absorption levels are shown in Table I. The average $K_a$ values calculated from the best-fitting $K_a$ values at each $B_1$ level are listed

[1] The authors gratefully acknowledge the use of the digital computer program NONLIN, which was supplied by Dr. Carl M. Metzler, The Upjohn Co., Kalamazoo, MI 49001

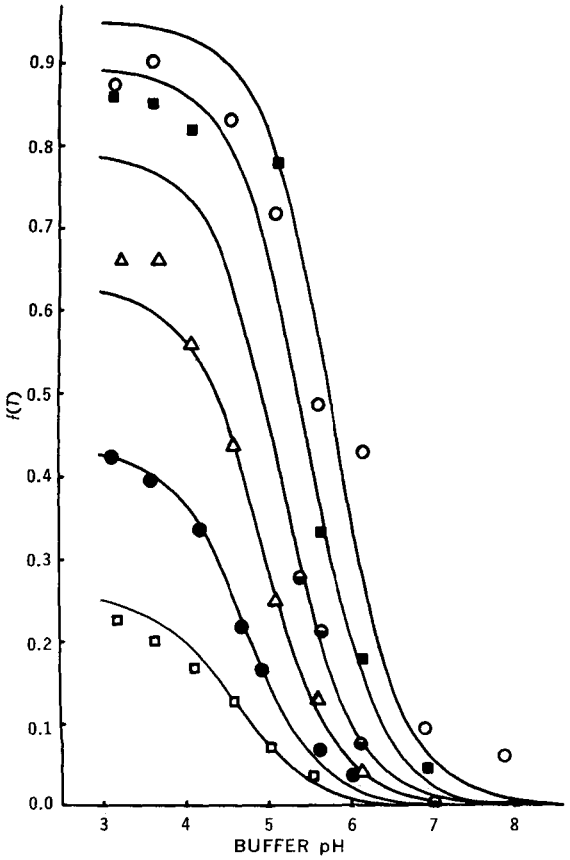


**Figure 2**—*Profiles of buccal absorption rate function* f(T) versus *buffer pH for the solutions of* p-n-*alkyl phenylacetic acids with* $B_1$ = *0.393 min.*$^{-1}$. *Solid curves are optimum* $f(T)_{theor}$ versus *buffer pH for the corresponding* $f(T)_{expt}$ *points shown for each acid. Key:* ○, *pentyl;* ■, *butyl;* ◒, *propyl;* △, *ethyl;* ●, *methyl; and* □, *H.*

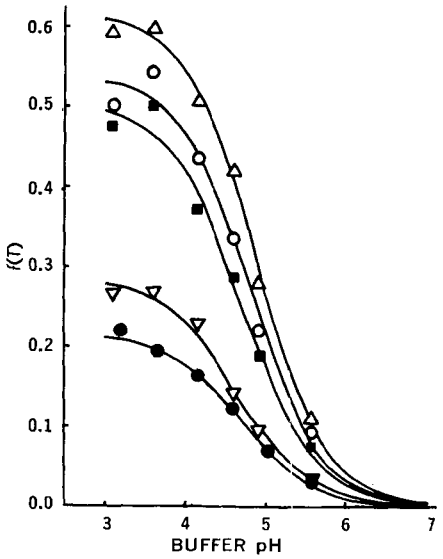


**Figure 3**—*Profiles of buccal absorption rate function* f(T) versus *buffer pH for the solutions of* p-*halogen phenylacetic acids with* $B_1$ = *0.408 min.*$^{-1}$. *Solid curves are optimum* $f(T)_{theor}$ versus *buffer pH for the corresponding* $f(T)_{expt}$ *points shown for each acid. Key:* △, *iodo;* ○, *bromo;* ■, *chloro;* ▽, *fluoro; and* ●, *H.*

at the bottom of Table I. These average $K_a$ values were used as fixed $K_a$ values for the whole series at each $B_1$ level. Then, by using the subroutine DFUNC, best-fitting $T_{comp}$ values were obtained for each member acid shown in Table II.

Although it was possible to average the best-fitting computer-given $K_a$ values in this case since the values reported in the literature for *p*-alkyl phenylacetic acids at 25° are fairly close (5), the actual computer-given $K_a$ values of phenylacetic acid, *p*-*n*-propylphenylacetic acid, and *p*-*n*-pentylphenylacetic acid were not included in the averaging of $K_a$ values for the following reasons. The phenylacetic acid cannot be classified as *p*-alkyl phenylacetic acid. The availability of *p*-*n*-propylphenylacetic acid data only at the high pH range (Fig 1A), where the transport is mainly membrane controlled, gave biased results. The computer-given $K_a$ values for *p*-*n*-pentylphenylacetic acid did not fit the rank order because its experimental values exhibited significant scatter from the smooth curve shown in Fig. 1A.

Then the *n* values for each $B_1$ level were calculated from the best-fitting $T_{comp}$ values, using Eq. 5 according to Step 6 of Part A of Scheme I. The average *n* values obtained in this manner ranged from 2.713 to 1.628 (Table II).

Part B of Scheme I deals with the selection of the best reference compound (one member of the series in the study). The procedure involves using the *n* value found from Part A, calculating $T_{theor}$ and $f(T)_{theor}$ for the other members of the series, and then determining which reference compound gives the best-fitting $f(T)_{theor}$ *versus* pH profiles for the entire series at the selected $B_1$ level. The family of such theoretical $f(T)$ *versus* pH profiles at a suitable $B_1$ level will demonstrate the validity of the model and its relevance to the reported experimental data of Beckett and Moffat (4).

When the data for every $B_1$ level reported in Table II ($T_{comp}$ values) were subjected to Part B of Scheme I, the $T_{comp}$ value of *p*-*n*-propylphenylacetic acid was found to be the best reference point with which to start. The theoretical $f(T)_{theor}$ *versus* pH profiles based on these results at $B_1$ = 0.393 min.$^{-1}$ are plotted in Fig. 2.

The solid curves are theoretical profiles consistent with Eq. 3, and the plotted points are the reported experimental results converted to $f(T)_{expt}$ values using Eq. 1. Figure 2 exhibits the best calculated fit among the experimental and predicted values at the best estimated maximum absorption level. The $f(T)_{theor}$ value of *p*-*n*-pentylphenylacetic acid in the region of pH 3 approaches unity, indicating thereby its almost maximum absorption tendency in the series. The *p*-*n*-hexylphenylacetic acid will not be expected to show any significant increase in the rate of buccal absorption over *p*-*n*-pentylphenylacetic acid at low pH. Thus, the prescribed model proves consistent for this series of compounds.

***p*-Halogen Phenylacetic Acids**—The preliminary examination of Fig. 1B reveals that the percentage of *p*-halogen phenylacetic acids absorbed within the pH range of 3–7 increases as the atomic weight of the halogen atom increases. Beckett and Moffat (4) concluded that when compared with *p*-alkyl phenylacetic acids, chlorine increases buccal absorption to approximately the same extent as a methyl group and iodine increases it equivalent to an ethyl group, but fluoro and bromo groups are about half as effective in increasing absorption as the chloro and iodo atoms, respectively.

**Table III**—Best-Fitting $T_{expt}$ and $K_a$ Values Obtained by the Use of the NONLIN Computer Program for Buccal Absorption Data of Phenylacetic and *p*-Halogen Phenylacetic[a] Acids

| Acid | $B_1$, min.$^{-1}$ 0.277 | 0.322 | 0.408 | 0.460 | 0.599 |
|---|---|---|---|---|---|
| **Best-Fitting $T_{expt}$** | | | | | |
| Phenylacetic | 2.145 | 2.667 | 3.630 | 4.248 | 5.829 |
| *p*-Fluorophenylacetic | 1.391 | 1.774 | 2.517 | 2.975 | 4.164 |
| *p*-Chlorophenylacetic | 0.347 | 0.564 | 0.983 | 1.238 | 1.911 |
| *p*-Bromophenylacetic | 0.260 | 0.463 | 0.855 | 1.093 | 1.724 |
| *p*-Iodophenylacetic | 0.104 | 0.282 | 0.625 | 0.835 | 1.387 |
| **Best-Fitting $K_a \times 10^5$** | | | | | |
| Phenylacetic | 3.018 | 2.826 | 2.626 | 2.503 | 2.370 |
| *p*-Fluorophenylacetic | 3.935 | 3.605 | 3.218 | 3.045 | 2.847 |
| *p*-Chlorophenylacetic | 7.651 | 5.472 | 3.971 | 3.567 | 3.007 |
| *p*-Bromophenylacetic | 7.812 | 5.101 | 3.494 | 3.092 | 2.559 |
| *p*-Iodophenylacetic | 14.624 | 6.276 | 3.578 | 2.977 | 2.334 |
| **Calculated $A$ Values[b]** | | | | | |
| *p*-Halogen phenylacetic acids | 0.462 | 0.091 | 0.004 | 0.006 | 0.029 |

[a] Literature values for $K_a$ at 25° (5): phenylacetic acid, $4.88 \times 10^{-5}$; *p*-fluorophenylacetic acid, $5.68 \times 10^{-5}$; *p*-chlorophenylacetic acid, $6.45 \times 10^{-5}$; *p*-bromophenylacetic acid, $6.49 \times 10^{-5}$; and *p*-iodophenylacetic acid, $6.93 \times 10^{-5}$. [b] These values were calculated by the use of Eq. 6.

Table IV—Lipid–Aqueous Partition Incremental Values, Calculated by Two Different Methods, for *p*-Halogen Phenylacetic Acids at Various Assumed $B_l$ Levels[a]

| Acid | $B_l$ = 0.277 min.$^{-1}$ | | $B_l$ = 0.322 min.$^{-1}$ | | $B_l$ = 0.408 min.$^{-1}$ | | $B_l$ = 0.460 min.$^{-1}$ | | $B_l$ = 0.599 min.$^{-1}$ | |
|---|---|---|---|---|---|---|---|---|---|---|
| | $n$ | $n^*$ | $n$ | $n^*$ | $n$ | $n^*$ | $n$ | $n^*$ | $n$ | $n^*$ |
| *p*-Fluorophenylacetic | 1.542 | 1.602 | 1.495 | 1.553 | 1.442 | 1.489 | 1.428 | 1.458 | 1.400 | 1.428 |
| *p*-Chlorophenylacetic | 6.175 | 5.990 | 4.703 | 4.583 | 3.691 | 3.607 | 3.431 | 3.343 | 3.051 | 2.982 |
| *p*-Bromophenylacetic | 8.241 | 7.704 | 5.729 | 5.893 | 4.243 | 4.336 | 3.885 | 3.946 | 3.382 | 3.438 |
| *p*-Iodophenylacetic | 20.604 | 22.289 | 9.416 | 9.981 | 5.804 | 6.076 | 5.087 | 5.253 | 5.753 | 4.331 |

[a] Values for $n$ and $n^*$ obtained by the use of Eqs. 5 and 8, respectively.

To investigate whether our physical model approach would yield similar results in terms of the incremental constant, it was decided to subject the above data to the physical model presented earlier.

Because of the differences among the pKa (25°) values reported in the literature (5) (*i.e.*, phenylacetic acid, 4.312; *p*-fluorophenylacetic acid, 4.246; *p*-chlorophenylacetic acid, 4.190; *p*-bromophenylacetic acid, 4.188; and *p*-iodophenylacetic acid, 4.177), it was decided not to average out the pKa (or $K_a$) values for the series. Since it was not possible to follow exactly Part A of Scheme I, the calculations were carried out in the following manner. From the experimental data points shown in Fig. 1B, the values for $K_u$ were calculated. Thereafter, the corresponding $f(T)_{expt}$ values were calculated using the same range of $B_l$ used for the *p*-*n*-alkyl phenylacetic acid series, because $B_l$ is descriptive of the permeability of the drug across the aqueous diffusion layer. The subroutine DFUNC of the NONLIN program was then utilized to obtain best-fitting $T_{expt}$ and $K_a$ values for the $f(T)_{expt}$ values calculated. From the best-fitting $T_{expt}$ values, the incremental constant, $n$, henceforth named substituent constant for halogen derivatives, was calculated from Eq. 5. The results of these calculations are shown in Table III.

The next step was the determination of the best estimate of $B_l$, and this was accomplished by obtaining values for the following expression at every assumed $B_l$ level:

$$A = \sum_{F}^{I} (\mathrm{pKa_{theor}} - \mathrm{pKa_{expt}})^2 \qquad \text{(Eq. 6)}$$

The value of $A$ from Eq. 6 will demonstrate the closeness of the fit between the theoretically derived and the experimental values given by the computer as best fits. Therefore, the best maximum absorption level would be the one with the lowest value of $A$ among all assumed levels of $B_l$.

The $\mathrm{pKa_{expt}}$ values for Eq. 6 were obtained from the best-fitting $K_a$ values given by the computer, and the $\mathrm{pKa_{theor}}$ values were obtained by the use of the following expressions:

$$\mathrm{pKa_{theor}}\ (\text{fluoro derivative}) = \mathrm{pKa_{expt}}\ (\text{phenylacetic acid}) - 0.066 \qquad \text{(Eq. 7}a\text{)}$$

$$\mathrm{pKa_{theor}}\ (\text{chloro derivative}) = \mathrm{pKa_{expt}}\ (\text{phenylacetic acid}) - 0.122 \qquad \text{(Eq. 7}b\text{)}$$

$$\mathrm{pKa_{theor}}\ (\text{bromo derivative}) = \mathrm{pKa_{expt}}\ (\text{phenylacetic acid}) - 0.124 \qquad \text{(Eq. 7}c\text{)}$$

$$\mathrm{pKa_{theor}}\ (\text{iodo derivative}) = \mathrm{pKa_{expt}}\ (\text{phenylacetic acid}) - 0.135 \qquad \text{(Eq. 7}d\text{)}$$

These relationships were obtained from the reported literature pKa (25°) values of phenylacetic acid and its halogen derivatives (5). The reference $\mathrm{pKa_{expt}}$ (phenylacetic acid) for these expressions was the best-fitting pKa value of phenylacetic acid given by the computer.

The examination of the values of A (Table III) reveals the trend of reduction in the value as one increases $B_l$ up to 0.408. The minimum value is at the level of $B_l$ = 0.408. The values of the substituent constant, $n$, obtained by the use of Eq. 5 were compared with the following expression, which was derived from Eqs. 3 and 5:

$$n = \frac{[1 - f(T)_{pa}]f(T)_{px}}{[1 - f(T)_{px}]f(T)_{pa}} \cdot \frac{[1 + K_{apx}/(\mathrm{H^+})]}{[1 + K_{apa}/(\mathrm{H^+})]} \qquad \text{(Eq. 8)}$$

where subscripts *pa* and *px* stand for phenylacetic acid and *p*-halogen phenylacetic acid, respectively. The $f(T)$ values in Eq. 8 are $f(T)_{expt}$ for the respective compounds, and the $K_a$ values are the computer-given best-fitting values. The value of $n$ obtained by the use of Eq. 8 is the substituent effect observed between two experimental absorption data points at the same buffer pH. The comparison of $n$ values obtained by the use of Eqs. 5 and 8 at all maximum absorption levels points out the similarity in these values for each *p*-halogen phenylacetic acid. These values at selected levels of $B_l$ are shown in Table IV. As one is inclined to select the values at $B_l$ = 0.408 min.$^{-1}$, these results differ somewhat from the conclusions drawn by Beckett and Moffat (4). The values derived come closer to the increase in partition coefficient values reported

Table V—Buccal Absorption Data of Substituted Benzoic Acids Treated in Accordance with the Physical Model[a] Equations

| Acid | $B_l$, min.$^{-1}$ 0.322 | 0.379 | 0.408 | 0.460 | 0.599 |
|---|---|---|---|---|---|
| **Best-Fitting $T_{expt}$** | | | | | |
| Benzoic | 0.286 | 0.516 | 0.631 | 0.841 | 1.395 |
| *o*-Toluic | 0.264 | 0.490 | 0.603 | 0.809 | 1.353 |
| *m*-Toluic | 0.145 | 0.350 | 0.452 | 0.637 | 1.132 |
| *p*-Toluic | 0.008 | 0.144 | 0.231 | 0.389 | 0.807 |
| **Best-Fitting $K_a \times 10^5$** | | | | | |
| Benzoic | 13.857 | 9.071 | 7.945 | 6.732 | 5.279 |
| *o*-Toluic | 17.118 | 10.888 | 9.497 | 7.988 | 6.239 |
| *m*-Toluic | 14.245 | 6.952 | 5.785 | 4.640 | 3.384 |
| *p*-Toluic | 97.714 | 9.886 | 6.634 | 4.432 | 2.787 |
| **Calculated $n$ Values[b]** | | | | | |
| *o*-Toluic | 1.083 | 1.053 | 1.047 | 1.039 | 1.031 |
| *m*-Toluic | 1.975 | 1.476 | 1.398 | 1.321 | 1.233 |
| *p*-Toluic | 36.746 | 3.579 | 2.738 | 2.161 | 1.729 |
| **Calculated $A$ Values[b]** | | | | | |
| Toluic acids | 0.987 | 0.078 | 0.058 | 0.057 | 0.076 |

[a] Literature values for $K_a$ at 25° (5): benzoic acid, $6.27 \times 10^{-5}$; *o*-toluic acid, $12.35 \times 10^{-5}$; *m*-toluic acid, $5.35 \times 10^{-5}$; and *p*-toluic acid, $4.24 \times 10^{-5}$. [b] Values for $n$ and $A$ calculated by the use of Eqs. 5 and 6, respectively.

Table VI—Summary of Incremental Partition Constants for Various Functional Groups on Certain Parent Acidic Compounds

| Acid | $B_l$, min.$^{-1}$ | Incremental Partition Constant $n$ |
|---|---|---|
| *p*-Alkyl phenylacetic | 0.393 | 2.22 for $CH_2$ |
| Phenylacetic/*p*-methylphenylacetic | 0.393 | 2.22 for *p*-$CH_3$ |
| Phenylacetic/*p*-halogen phenylacetic | 0.408 | 1.47 for F<br>3.65 for Cl<br>4.29 for Br<br>5.94 for I |
| Benzoic/toluic | 0.408 | 1.05 for *o*-$CH_3$<br>1.40 for *m*-$CH_3$<br>2.74 for *p*-$CH_3$ |
| *n*-Alkanoic | 0.416 | 2.33 for $CH_2$[a] |

[a] Obtained from *Reference 1*.

**Table VII**—Incremental Effect of Either Addition or Substitution of a Methylene Group, a Methyl Group, or a Halogen Atom upon the Partition Coefficients of Selected Acidic Compounds in Organic Solvent–Water Systems Reported in the Literature

| From the Data of Collander (3) | Increase in Partition Coefficient in Isobutanol–Water System[a] |
|---|---|
| Methylene group increment within series: | |
| Acetic acid → caproic acid | 2.8 |
| Methyl acetate → ethyl acetate | 2.8 |
| Bromoacetic acid → bromobutyric acid | 2.8 |
| Malonic acid → diethylmalonic acid | 2.6 |
| Malonic acid → azelaic acid | 2.1 |
| Succinic acid → adipic acid | 1.9 |
| Average | 2.5 |
| Halogen substitution effect: | |
| Chloroacetic acid/acetic acid | 2.2 |
| α-Bromobutyric acid/butyric acid | 3.6 |
| Bromoacetic acid/acetic acid | 3.1 |
| α-Bromopropionic acid/propionic acid | 3.5 |
| Iodoacetic acid/acetic acid | 4.9 |

| From the Data of Hansch *et al.* (7–9) | Increase in Partition Coefficient in Octanol–Water System[b] |
|---|---|
| Methylene group increment within series | 3.16 |
| Halogen substitution effect: | |
| *p*-Fluorophenoxyacetic acid/phenoxyacetic acid | 1.58 |
| *p*-Chlorophenoxyacetic acid/phenoxyacetic acid | 5.01 |
| *p*-Bromophenoxyacetic acid/phenoxyacetic acid | 10.47 |
| *p*-Iodophenoxyacetic acid/phenoxyacetic acid | 18.20 |
| Methyl group substitution effect: | |
| *m*-Methylbenzoic acid/benzoic acid | 0.56 |
| *p*-Methylbenzoic acid/benzoic acid | 0.46 |
| *o*-Methylphenoxyacetic acid/phenoxyacetic acid | 4.79 |
| *m*-Methylphenoxyacetic acid/phenoxyacetic acid | 3.24 |
| *p*-Methylphenoxyacetic acid/phenoxyacetic acid | 3.31 |

| From the Data of Beckett and Moffat (10): | Increase in Partition Coefficient in *n*-Heptane–0.1 *N* HCl System[a] |
|---|---|
| Methylene group increment effect: | |
| ——*n*-Alkanoic acids—— | |
| *n*-Hexanoic acid/*n*-valeric acid | 2.75 |
| *n*-Heptanoic acid/*n*-hexanoic acid | 3.91 |
| *n*-Octanoic acid/*n*-heptanoic acid | 4.51 |
| *n*-Nonanoic acid/*n*-octanoic acid | 2.59 |
| *n*-Decanoic acid/*n*-nonanoic acid | 2.43 |
| *n*-Undecanoic acid/*n*-decanoic acid | 1.52 |
| *n*-Dodecanoic acid/*n*-undecanoic acid | 5.18 |
| Average | 3.27 |
| ——*p*-Alkyl phenylacetic acids—— | |
| *p*-Ethylphenylacetic acid/*p*-methylphenylacetic acid | 2.10 |
| *p*-*n*-Propylphenylacetic acid/*p*-ethylphenylacetic acid | 3.00 |
| *p*-*n*-Butylphenylacetic acid/*p*-*n*-propylphenylacetic acid | 5.32 |
| *p*-*n*-Pentylphenylacetic acid/*p*-*n*-butylphenylacetic acid | 5.45 |
| *p*-*n*-Hexylphenylacetic acid/*p*-*n*-pentylphenylacetic acid | 1.65 |
| Average | 3.50 |
| Halogen substitution effect: | |
| *p*-Fluorophenylacetic acid/phenylacetic acid | 1.0 |
| *p*-Chlorophenylacetic acid/phenylacetic acid | 6.0 |
| *p*-Bromophenylacetic acid/phenylacetic acid | 9.0 |
| *p*-Iodophenylacetic acid/phenylacetic acid | 12.0 |
| Methyl group substitution effect: | |
| *o*-Methylbenzoic acid/benzoic acid | 2.27 |
| *m*-Methylbenzoic acid/benzoic acid | 2.82 |
| *p*-Methylbenzoic acid/benzoic acid | 2.09 |
| 2,4-Dimethylbenzoic acid/benzoic acid | 8.00 |
| 2,6-Dimethylbenzoic acid/benzoic acid | 0.90 |
| 2,4,6-Trimethylbenzoic acid/benzoic acid | 31.36 |
| 2,3,5,6-Tetramethylbenzoic acid/benzoic acid | 31.09 |

[a] Increase in partition coefficient = partition coefficient of derivative/partition coefficient of parent compound. [b] Equivalent to the antilogarithmic value of Hansch's $\pi$ constant.

by Collander (3) for isobutanol–water systems in the same rank order fashion.

The theoretical $f(T)$ *versus* buffer pH profiles for *p*-halogen phenylacetic acids based on the model equation at $B_1 = 0.408$ min.$^{-1}$ level are presented in Fig. 3.

**Substituted Benzoic Acids**—In this section the physical model approach is applied to the buccal absorption data presented in Figs. 1C and 1D, namely, benzoic acid as the parent molecule and toluic acids as the substituted benzoic acids. It is hoped that the calculated lipid–aqueous incremental constant, $n$, henceforth named as positional substituent constant for these compounds, will demonstrate the effect of a methyl group substitution on the *ortho*-, *meta*-, and *para*-positions of the phenyl ring of the benzoic acid molecule.

The analytical treatment of the data followed the identical scheme used previously for the *p*-halogen phenylacetic acid series. As shown in Table V, the best set of $T_{expt}$, $K_a$, and $n$ was obtained with $B_1$ equal to 0.408 min.$^{-1}$ and was used to determine the theoretical $f(T)$ by Eq. 3. In Fig. 4 the theoretical $f(T)$ *versus* buffer pH profiles are compared with the experimental results. One does not observe any significant difference in the absorption rate from benzoic acid to *o*-toluic acid, since the incremental constant of the *o*-methyl group was nearly unity. However, the substitution of the methyl group in the *meta*- or *para*-position improves the absorption rate.

A list of the values of the incremental partition constant, $n$, calculated by the physical model approach for the above-mentioned series of compounds is presented in Table VI. To present a comparative evaluation of the lipid–aqueous partition incremental constants for similar acids, the values obtained from literature are

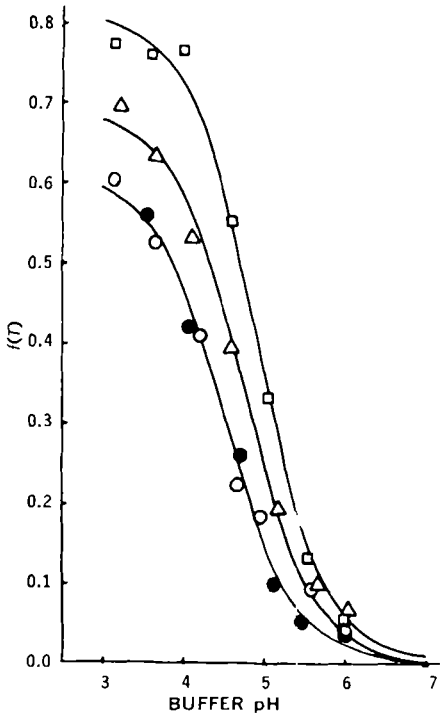


**Figure 4**—*Profiles of buccal absorption rate function* f(T) versus *buffer pH for the solutions of methyl-substituted benzoic acids with* $B_1 = 0.408$ *min.*$^{-1}$. *Solid curves are optimum* $f(T)_{theor}$ versus *buffer pH for the corresponding* $f(T)_{expt}$ *points shown for each acid. Key:* □, p-*toluic;* △, m-*toluic;* ●, o-*toluic; and* ○, *benzoic acid.*

tabulated in Table VII. As can be seen in Table VII, the average increase in partition coefficient due to a methylene group addition within a linear homologous series of acids has similar values if one selects either the octanol–water or *n*-heptane–0.1 *N* hydrochloric acid system. This is in disagreement with the position constants obtained from the buccal absorption analysis. It would indeed be interesting if partitioning data with the isobutanol–water system were available.

Although one may obtain some information about the transport of nonionized drug molecules across the buccal membrane by the use of the regression equation suggested by Lien *et al.* (6) as a one-point comparison at any one particular pH, the physical model Eqs. 1–4 suggested in this report can provide absorption profiles of each acidic drug for the entire experimental buffer pH range.

The data presented here provide further evidence that the diffusion model suggested earlier by Ho and Higuchi (1) for buccal absorption is consistent in the cases of *p*-alkyl phenylacetic, *p*-halogen phenylacetic, and toluic acids. The model underscores the importance of the diffusion layer and its effect on the transport of nonionized drug molecules in the buccal absorption situation.

## REFERENCES


(1) N. F. H. Ho and W. I. Higuchi, *J. Pharm. Sci.*, **60,** 537 (1971).

(2) A. H. Beckett and A. C. Moffat, *J. Pharm. Pharmacol.*, **20,** 239S(1968).

(3) R. Collander, *Acta Chem. Scand.*, **4,** 1085(1950).

(4) A. H. Beckett and A. C. Moffat, *J. Pharm. Pharmacol.*, **21,** 139S(1969).

(5) G. Kortum, W. Vogel, and K. Andrussow, "Dissociation Constants of Organic Acids in Aqueous Solution," Butterworths, London, England, 1961.

(6) E. J. Lien, R. T. Koda, and G. L. Tong, *Drug Intel. Clin. Pharm.*, **5,** 38(1971).

(7) C. Hansch, R. M. Muir, T. Fujita, P. M. Maloney, F. Geiger, and M. Streich, *J. Amer. Chem. Soc.*, **85,** 2817(1963).

(8) C. Hansch and T. Fujita, *ibid.*, **86,** 1616(1964).

(9) C. Hansch and E. Coats, *J. Pharm. Sci.*, **59,** 731(1970).

(10) A. H. Beckett and A. C. Moffat, *J. Pharm. Pharmacol.*, **21,** 144S(1969).


## ACKNOWLEDGMENTS AND ADDRESSES


Received April 21, 1972, from the *College of Pharmacy, University of Michigan, Ann Arbor, MI 48104*

Accepted for publication June 27, 1972.

Supported in part by National Institutes of Health Research Grant GM 13368 and by a research grant from Pfizer, Inc., New York, N. Y.



▲ To whom inquiries should be directed.


# Biopharmaceutical Studies on Aminoethanesulfonylphenetidine and Related Compounds III: Drug in Blood


**SHUN-ICHI NAITO▲ and KAZUO FUKUI**



**Abstract** □ No effects of taurinophenetidine and nicotinoyltaurinophenetidine on erythrocytolysis and methemoglobin production were observed. It was also found that about 40% of the nicotinoyltaurinophenetidine, which is absorbed after its oral administration, is hydrolyzed in the blood of rabbits, rats, and mice.



**Keyphrases** □ Aminoethanesulfonylphenetidine—effect on erythrocytolysis and methemoglobin production, plasma levels in rabbits □ Taurinophenetidine—effect on erythrocytolysis and methemoglobin production, plasma levels in rabbits □ Nicotinoylaminoethanesulfonylphenetidine—effect on erythrocytolysis and methemoglobin production, blood levels in rabbits, rats, mice □ Nicotinoyltaurinophenetidine—effect on erythrocytolysis and methemoglobin production, blood levels in rabbits, rats, mice


The binding ratio of aminoethanesulfonylphenetidine (taurinophenetidine) or nicotinoylaminoethanesulfonylphenetidine (nicotinoyltaurinophenetidine) with serum protein in rabbits and the excretion of taurinophenetidine and its nicotinoyl derivative in rat feces and in rat and rabbit bile were previously investigated (1). It was also observed that taurinophenetidine has some analgesic and antipyretic activities and that nicotinoyltaurinophenetidine has some analgesic and anti-inflammatory activities but no antipyretic action (1).

In the present study, the effect of taurinophenetidine and nicotinoyltaurinophenetidine on erythrocytolysis and methemoglobin production was examined to determine the toxicity of these drugs before undertaking clinical studies. The blood levels of nicotinoyltaurinophenetidine and its hydrolysis product following its oral administration to mice, rats, and rabbits were also investigated.

## EXPERIMENTAL

***In Vitro* Osmotically Induced Hemolytic Action**—The hemolytic effects of taurinophenetidine and nicotinoyltaurinophenetidine on rat blood were determined by the method reported by Okui and Uchiyama (2).

A suspension of 0.1 ml. of rat blood in 2 ml. of sodium chloride–sodium citrate solution (0.6 g. of sodium citrate in 100 ml. of 0.9% sodium chloride solution) was centrifuged for 2 min. The residue of blood corpuscles thus obtained was suspended in 2 ml. of 0.9% sodium chloride solution. After another centrifugation, the residue was again resuspended in 1 ml. of 0.9% sodium chloride solution and this suspension was used for the following procedures.

*Procedure A*—To 0.25 ml. of this suspension, 0.25 ml. of 0.2 *M* phosphate buffer (pH 7.4) was added and the mixture was incubated at 37 ± 2° for 15 min. After standing for 45 min. at room temperature, the mixture was centrifuged for 2 min. To 0.2 ml. of the supernate, 3.3 ml. of water was added and the absorbance at 550 nm. was determined.